HREM identification of "one-dimensionally-disordered" polytypes in the SiC (CVI) matrix of SiC/SiC composites

Sylvie Schamm-Chardon, Annie Mazel, Dominique Dorignac, Jean Sévely

Microsc. Microanal. Microstruct. **2** (1991) 59–73 FEBRUARY **1991,** PAGE 59

Classification
Physics Abstracts
61.16D — 81.15H

HREM identification of "one-dimensionally-disordered" polytypes in the SiC (CVI) matrix of SiC/SiC composites

Sylvie Schamm, Annie Mazel, Dominique Dorignac and Jean Sévely

CEMES-LOE/CNRS, B.P. 4347, 31055 Toulouse Cedex, France

(Received October 18, 1990, accepted December 17, 1990)

Résumé. — La matrice de carbure de silicium des composites SiC/SiC a été examinée d'un point de vue chimique et structural par spectroscopie de pertes d'énergie d'électrons (EELS) et par microscopie électronique à haute résolution (MEHR). La croissance colonnaire des cristaux de la matrice et leur distribution radiale par rapport aux fibres qui constituent le renfort sont caractéristiques de ce matériau. La stœchiométrie des cristaux a été vérifiée (Si/C = 1). La structure cubique (polytype 3C) de certains d'entre-eux a été identifiée à l'aide des diagrammes de diffraction. Dans le cas d'autres cristaux, dits "polytypes de désordre unidimensionnel", l'imagerie haute résolution s'est avérée nécessaire pour mettre en évidence la désorganisation dans la direction d'empilement des couches de tétraèdres. La résolution ponctuelle, 0,19 nm, du microscope PHILIPS CM30-ST, fonctionnant à 300 kV, permet de reconnaître la structure projetée de SiC et d'évaluer le degré de désordre dans ces polytypes. La simulation numérique des images nous a permis d'interpréter sans ambiguité nos clichés expérimentaux.

Abstract. — The matrix of SiC/SiC composites has been observed by electron energy loss spectroscopy (EELS) and high resolution electron microscopy (HREM) from both the chemical and the structural point of view. In this material, columnar growth and radial arrangement around the fibres of the reinforcement are typically observed for the crystal of the matrix. The ratio, Si/C = 1, of these crystals has been checked. The cubic structure of some of them has been identified through their diffraction patterns. High resolution experiments were performed to recognize the structure of the others polytypes, which are characterized by a disorder in the direction of the tetrahedral layer stacking. For this reason, they are called, "one-dimensionally-disordered" polytypes. The PHILIPS CM30-ST point resolution (0.19 nm) enables the projected SiC structure to be recognized so that the degree of disorder in this polytype can be estimated. The interpretation of the experimental images was based on comparison with simulations.

1. Introduction.

The fact that a composite made of two brittle constituents (ceramics) may not be brittle justifies the interest during recent years in ceramic matrix composites (CMC) [1]. Toughened CMC consisting of a fibrous preform embedded in a ceramic matrix are being developed as a potential solution to some of today's high temperature materials needs. Among them are SiC/SiC composites, the matrix of which is investigated in this paper.

The properties of CMC are governed by the characteristics of their different constituents, i.e. the fibre, the matrix and also the interface between them. The relationships between these properties and characteristics are not yet clearly understood. This could be remedied by characterizing simultaneously the microstructure of the constituents and the mechanical properties of the corresponding composite. Numerous models have already been developed to describe the mechanical behaviour of the CMC, but their microstructure has not been thoroughly investigated.

By using electron energy loss spectroscoy (EELS) and high resolution electron microscopy (HREM), it is possible to characterize materials from the chemical and the structural point of view at a quasi-atomic scale. The application of such studies to the different constituents of the CMC is now necessary for their development.

The reinforcement (Nicalon type fibres) and the interface in the SiC/SiC composites have already been observed at nanometric resolution [2-5], but the matrix has not hitherto been considered. The latter is obtained according to the Chemical Vapour Infiltration process (CVI). In this process, the open porosity of a fibrous preform is infiltrated by reactant gases that decompose at elevated temperature (about 1000° C) to deposit silicon carbide between and around the fibres [6]. The microstructure of the SiC(CVI) is strongly dependent on the numerous preparation parameters such as temperature, total pressure, gas composition and flow rate. This investigation was initiated to characterize the microstructure of the SiC matrix and to determine which of the SiC structural forms (polytypes) have been deposited during the CVI process. HREM was performed with JEOL 200CX-S and PHILIPS CM30-ST microscopes. In order to interpret the contrast of the experimental images correctly, they have been compared with simulated ones which take into account the various parameters involved in the high resolution experiments (voltage, defocus, thickness and orientation of the sample) [7].

2. Polytypism of silicon carbide.

The different polytypes of silicon carbide (more than 150 different forms) are all based upon a framework of SiC_4 (or CSi_4) tetrahedral units. These units are associated within layers by three of their vertices in the same way as hard spheres in a compact structure. Two succesive layers occupy positions which are related to one another either by a simple translation (cubic polytype 3C) or by both a translation and a rotation of 180° (hexagonal polytypes, e.g. 6H) (Fig. 1). Polytypism in silicon carbide results from the ability of the tetrahedral unit layers to be stacked according to different sequences on the basis of these two modes. All SiC polytypes have two structural parameters in common (that of the tetrahedral basal plane), $a = b = 0.308$ nm. They differ only by the third parameter, which is a multiple of the tetrahedral unit height (in the direction of the stacking sequence), i.e. $c = 0.25 \times N$ nm (Fig. 1). N is the periodicity of the polytype, that is to say the number of layers after which the stacking recurs. Short period polytypes, denoted 2H, 4H, 6H, 15R and 3C in the Ramsdell notation (H for hexagonal, R for rhombohedral, C for cubic), are called "basal structures" of SiC because polytypes of large c parameter can be constructed from stacking sequences of these polytypes.

When SiC is observed along a $< 11\bar{2}0 >$ (hexagonal structures) or $< 110 >$ (cubic structure) direction, it is possible to visualize the stacking sequence of the tetrahedral layers [8-12]. With such an orientation and for a high enough resolution of the microscope, the exact nature of each polytype can be identified. The point resolutions of the JEOL 200CX-S and PHILIPS CM30-ST microscopes are 0.27 and 0.19 nm, respectively. These values are sufficient to visualize the projected SiC bicolumns separated by 0.307 and 0.266 nm as shown in figure 1, which represents the projected interatomic distances of the tetrahedral units. However, the 0.109 nm distance between Si and C atomic columns cannot yet be resolved.

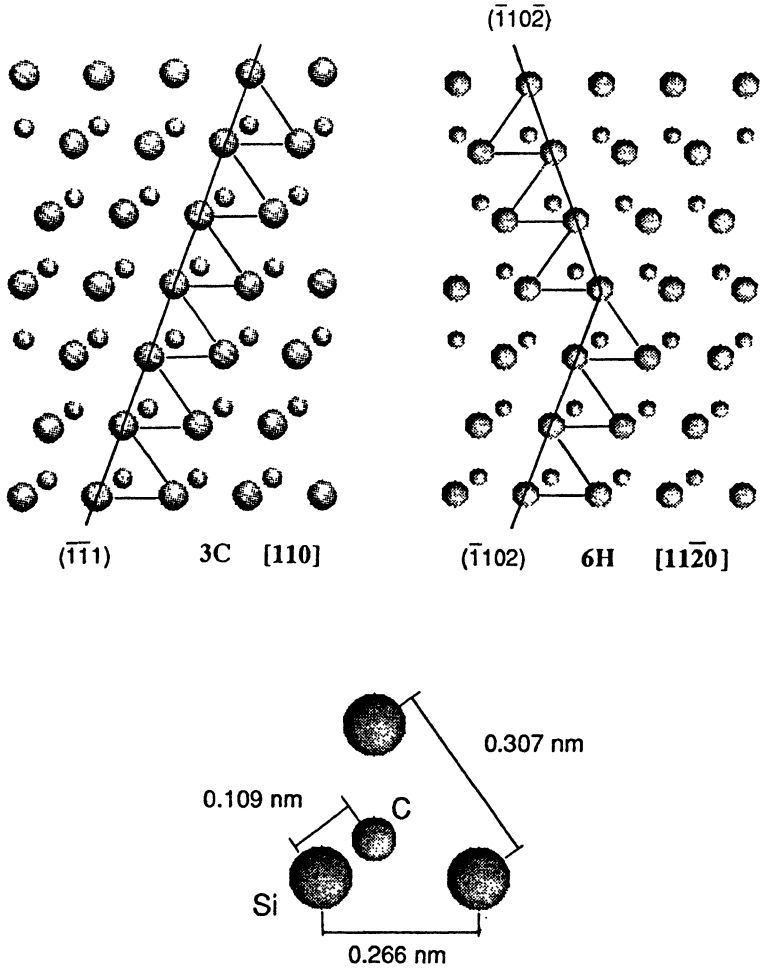

Fig. 1. — Structures of the cubic, 3C, and of one the hexagonal, 6H, forms of SiC respectively observed along the [110] and the [11$\bar{2}$0] direction. The corresponding interatomic distances are shown on the projected tetrahedral unit.

3. The SiC(CVI) matrix of SiC/SiC composites.

3.1 MICROSTRUCTURE. — The general morphology of the infiltrated matrix has ben observed in the conventional bright field image mode. Figure 2 shows such an image corresponding to an area located near the fibres constituting the preform of the composite. In this case, the fibres have their axes parallel to the incident beam and they have been eliminated during the ion milling operation. Their transversal sections were initially located where three circular holes are observed. The crystals of the SiC(CVI) matrix are columnar and grow radially from the surface of these fibres with some interruptions arising from the processing. Thus, the SiC(CVI) matrix appears as an arrangement of domains several micrometres across. They are delineated firstly by the boundaries between crystals grown from different fibres and secondly by several zones concentric with the transversal section of the fibres and related to a rupture of growth.

Three kinds of area are of interest in the SiC(CVI) matrix: the well-developed columnar crys-

Fig. 2. — Morphology of the SiC(CVI) matrix. The three holes of circular shape - two at the right bottom of the image and another one, but less visible, at the left bottom - were previously occupied by the transversal section of fibres. The three black arrows indicate the directions of growth of the SiC(CVI) crystals from the surface of the fibres.

tals, the boundary zones and the areas where a rupture of growth occurs. This paper is concerned only with crystals that have been studied both from the chemical and structural points of view.

3.2 COMPOSITION. — The ratio of the number of silicon and carbon atoms (N_{Si}/N_C) in the columnar crystals has been checked by EELS. This ratio has been determined by applying a quantitative treatment to the distributions corresponding to the Si-L edge to the C-K edge of the SiC(CVI) crystals and of a 6H single crystal, with proper thickness conditions, according to the following relation [13]:

$$R = \frac{N_{Si}}{N_C} = \frac{S_{Si}(\alpha, \Delta E)}{S_C(\alpha, \Delta E)} \cdot \frac{\sigma_C(\alpha, \Delta E)}{\sigma_{Si}(\alpha, \Delta E)}$$

where $S_{Si}(\alpha, \Delta E)$ and $S_C(\alpha, \Delta E)$ are the areas under the Si-L and the C-K distributions above the background (Fig. 3) and, $\sigma_{Si}(\alpha, \Delta E)$ and $\sigma_C(\alpha, \Delta E)$ are the partial cross-sections integrated over the collection angle α and the energy window ΔE. For the following experimental conditions, $V =$ 120 kV and $\alpha = 9.25$ mrad, the values of the partial cross-sections were: $\sigma_{Si} = 9.213 \times 10^{-20}$ cm^2 and $\sigma_C = 6.157 \times 10^{-21}$ cm^2. The value of the ratio obtained varies from 0.9 to 1.0 for the polytypes and is equal to 0.9 for the single crystal. Taking into account the 10% accuracy recognized for this kind of measurement, we can consider that the well-developed columnar crystals of the matrix are stoichiometric.

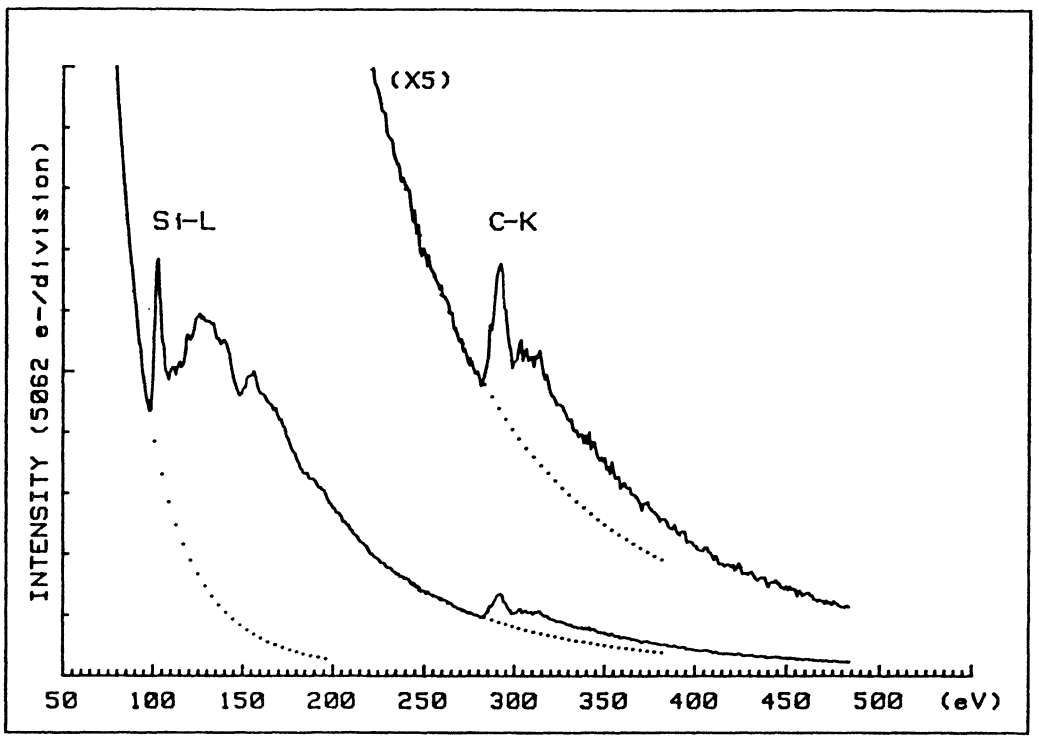

Fig. 3. — Electron Energy Loss spectra of a SiC(CVI) crystal ($V = 120$ kV, $\alpha = 9.25$ mrad). The dotted lines indicate the area under the Si-L and C-K edges above the background.

3.3 DIFFRACTION PATTERNS. — Two kinds of diffraction patterns have been obtained. The first corresponds to the cubic structure, which can be easily identified in this way. This structure may be perfect 3C structure (Fig. 4a), twinned (Fig. 4b) or heavily faulted (Fig. 4c). The second kind of diffraction patterns shows the same features as the heavily faulted cubic one (Fig. 5) but does not exhibit strong diffraction spots at the positions where they would be expected for the cubic structure ({111}, {002}). Here, the positions of the intensity maxima could be attributed to those of both the cubic and the hexagonal structures, as confirmed by the corresponding simulated diffraction patterns. From these patterns, the nature of the polytype cannot be directly identified, but the continuous streaking of the reflexions associated with the stacking direction indicates that the c parameter of this polytype is very large. Consequently, two assumptions can be proposed: either the stacking is ordered and the polytype has a very large period [14-16] or there is no periodicity and the polytype is called "one-dimensionally-disordered" [17-19].

3.4 HIGH RESOLUTION IMAGES. — High resolution images are dependent on numerous physical parameters, such as the microscope characteristics (i.e. voltage, spherical aberration and focus spread), the conditions of observation (i.e. defocus and beam divergence), and the sample itself (i.e. thickness and orientation). High resolution image interpretation is not straightforward. The best way of confirming these interpretations is to relate the experimental images to simulated ones [7, 20-22].

This procedure was followed in the case of the structure shown in figure 6, which has been extracted from an experimental image. This structure is observed along a $< 11\bar{2}0 >$ direction. It can be considered either as a large period polytype ($N = 30$) with $c = 7.5$ nm or as a part of a sequence of a "one-dimensionally-disordered" polytype. As shown in figure 6, the simulated diffraction pattern of this structure agrees perfectly wit the experimental one shown in figure 5.

The images of this polytype have been calculated for JEOL 200CX-S and PHILIPS CM30-ST microscopes with different thicknesses (5, 10, 15 and 20 nm) and defocus values corresponding to the two first positive and negative passbands (Figs. 7 and 8 respectively). They may be compared with the experimental images obtained with a JEOL microscope (Fig. 9) and with a PHILIPS microscope (Fig. 10).

Figure 9 is characterized by bands of different width perpendicular to the stacking direction. Some of these contain white dots, well separated, while others appear blurred. Such a feature is observed on nearly all the simulations corresponding to the 200 kV situation except for the 5 nm thickness (Fig. 7). It is noteworthy that these simulations were calculated for an axial illumination. The possible effect of a slight misalignment of the specimen [23] is only to emphasize such a feature as can be controled through calculations. No conclusion can be deduced about the exact nature of the polytype from such experiments.

As shown by the simulations, the problem could be solved if the resolution were better. This is confirmed by figure 10, which corresponds to an experiment on a CM30-ST microscope. From the comparison of simulations and figure 10 the image is consistent with a sample thickness of approximately 5 nm, with a defocus close to 78 nm. Figure 11, which is an enlargement of figure 10, emphasizes the excellent agreement between the experimental and the calculated images. Under these conditions, the white dots coincide exactly with the projected SiC atomic columns (see Fig. 1) and the nature of the stacking along the c direction can be directly identified. In the case of this SiC(CVI) crystal, no periodicity has been observed in the stacking over about a hundred nanometers. We can conclude that it is certainly a "one-dimensionally-disordered" polytype.

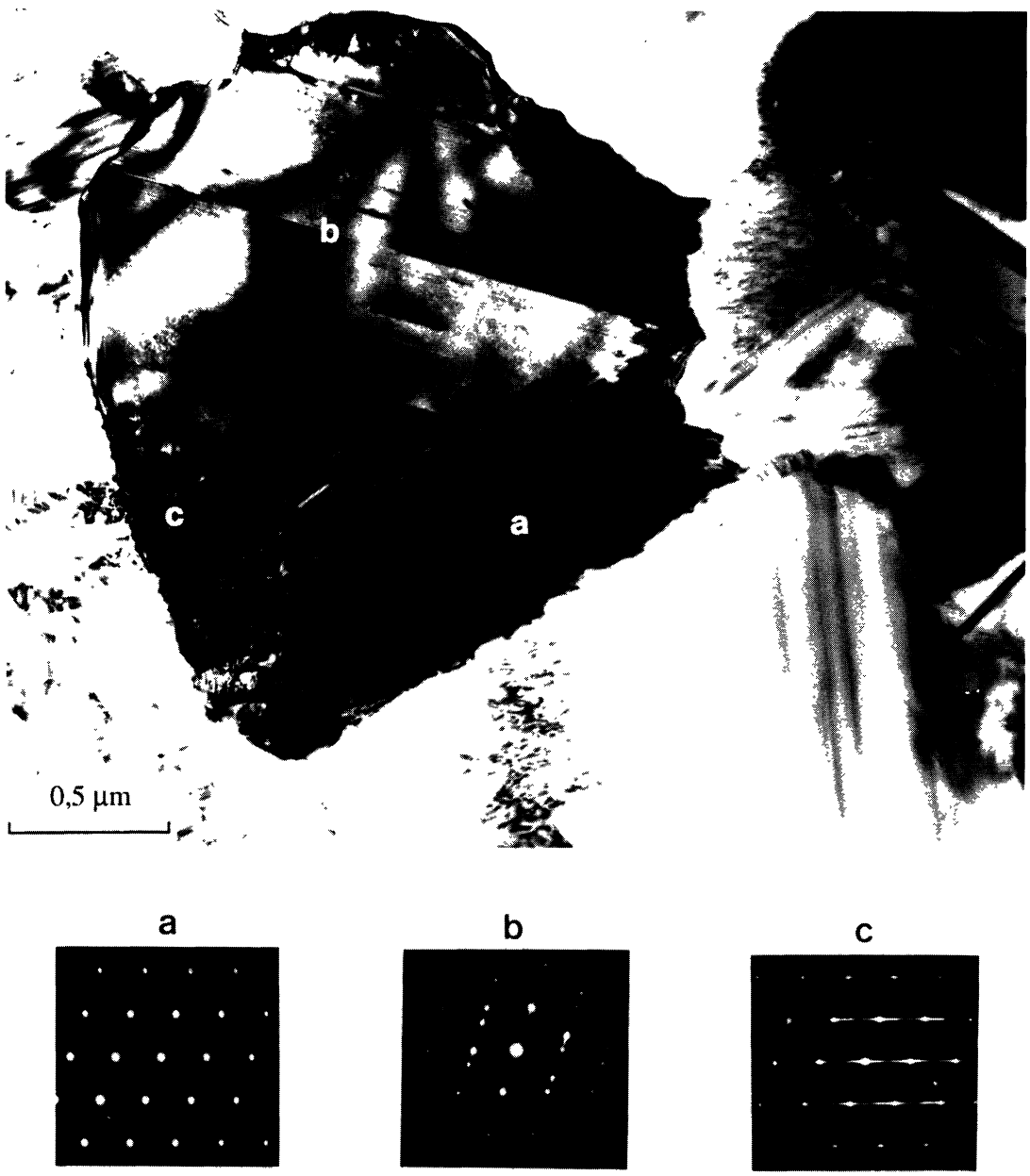

Fig. 4. — Bright field image and electron diffraction patterns of SiC(CVI) crystals oriented along a < 110 > direction. The perfect (a), twinned (b) and heavily faulted (c) 3C structures are observed.

4. Conclusion and discussion.

Perfect, twinned and heavily faulted cubic crystals have been easily identified in the SiC(CVI) matrix of SiC/SiC composites through their diffraction patterns.

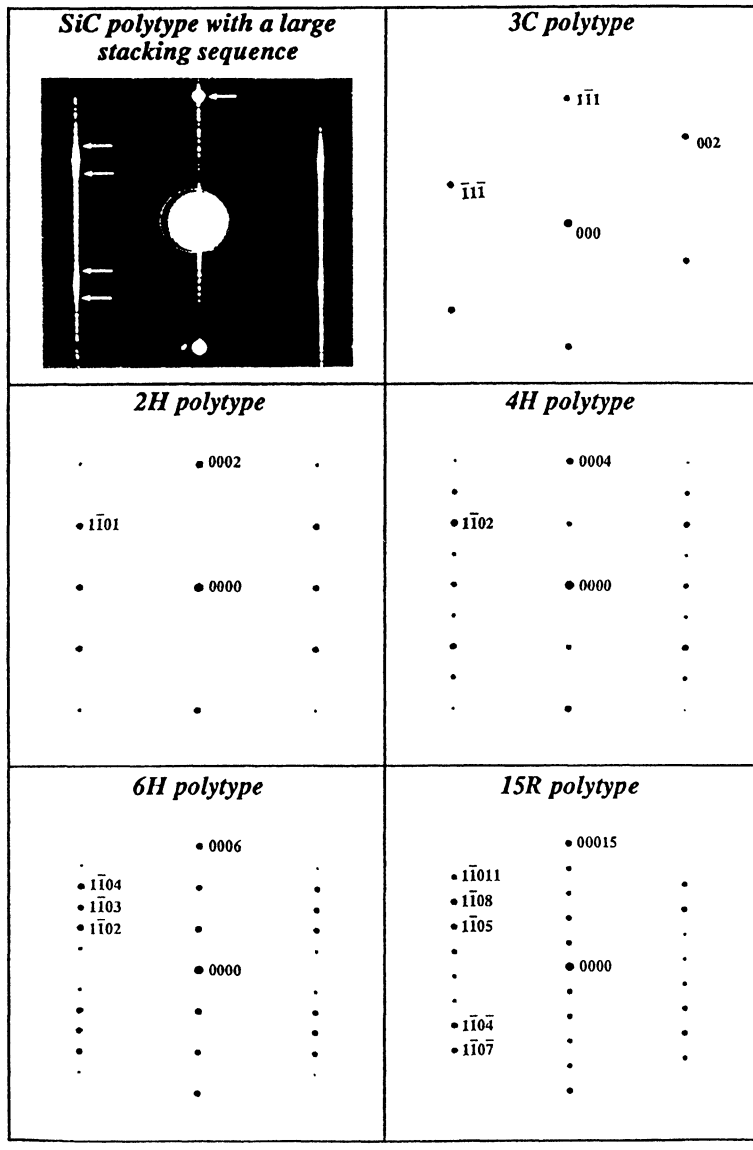

Fig. 5. — Simulated (3C, 2H, 4H, 6H and 15R) and experimental (SiC(CVI) crystal) diffraction patterns of SiC. The intensity maxima of the SiC(CVI) (indicated by arrows) can be attributed to those of both the cubic and the hexagonal forms of SiC (indexed on the corresponding simulated diffraction pattern).

"One-dimensionally-disordered" polytypes have also been identified in another area of the matrix by HREM experiments and calculations. Such polytypes were previously observed in 1978 by Shinozaki *et al.* in chemical vapour-deposited silicon carbide [17-19]. When imaged with about 1 nm resolution, these polytypes appear as a distribution of lamellae perpendicular to the growing direction. Today, the performance of modern high resolution electron microscopes, whose resolution is better than 0.2 nm, associated with image simulation, render the stacking sequence of disordered polytypes directly interpretable.

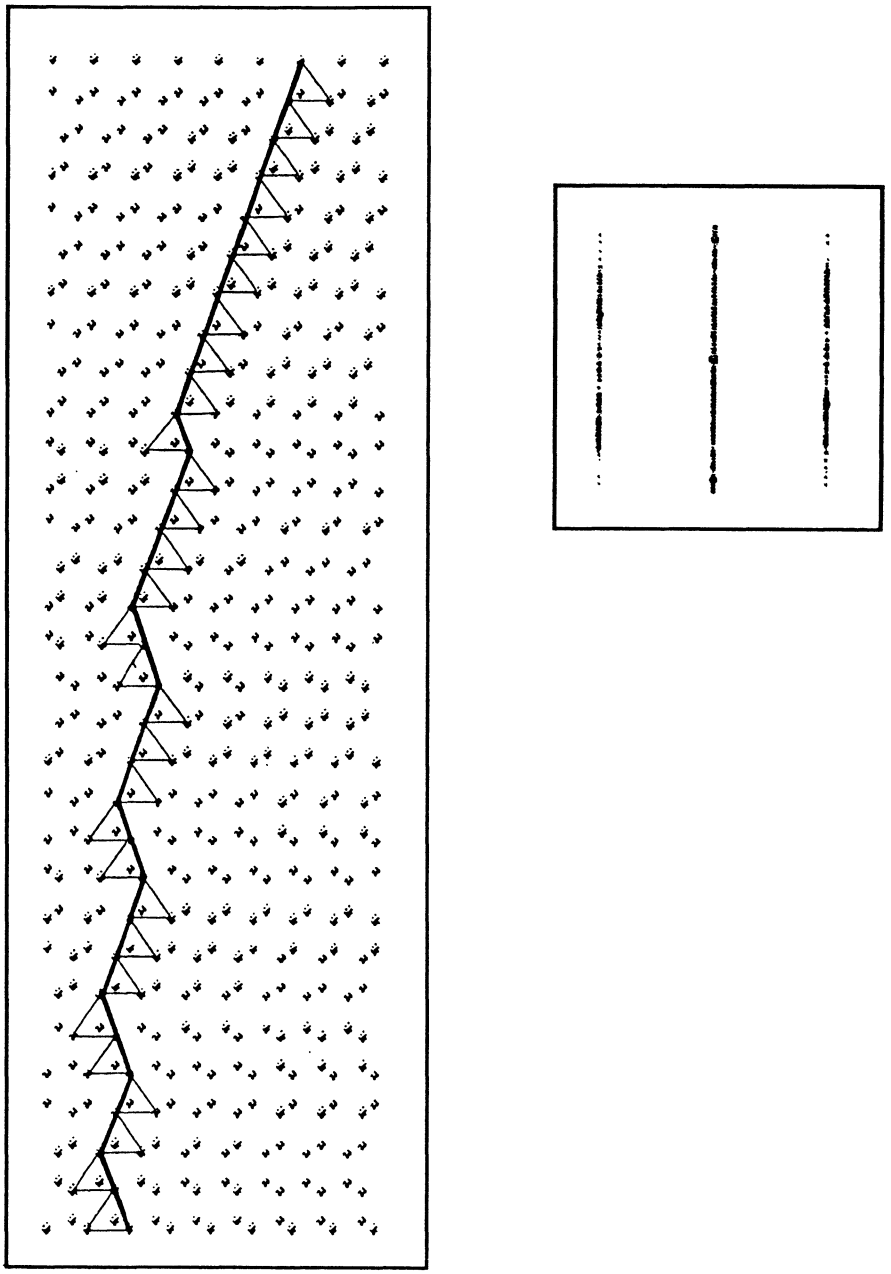

Fig. 6. — Structure extracted from an experimental image (Fig. 10 and 11) and the corresponding simulated diffraction pattern.

This new situation encourages us to go further in the understanding of the apparent irregularity in the stacking of the tetrahedral layers of these polytypes. Such an arrangement appears chaotic. The possibility of following directly the stacking order, using high resolution images, is one way of giving a quantitative description of this type of arrangement.

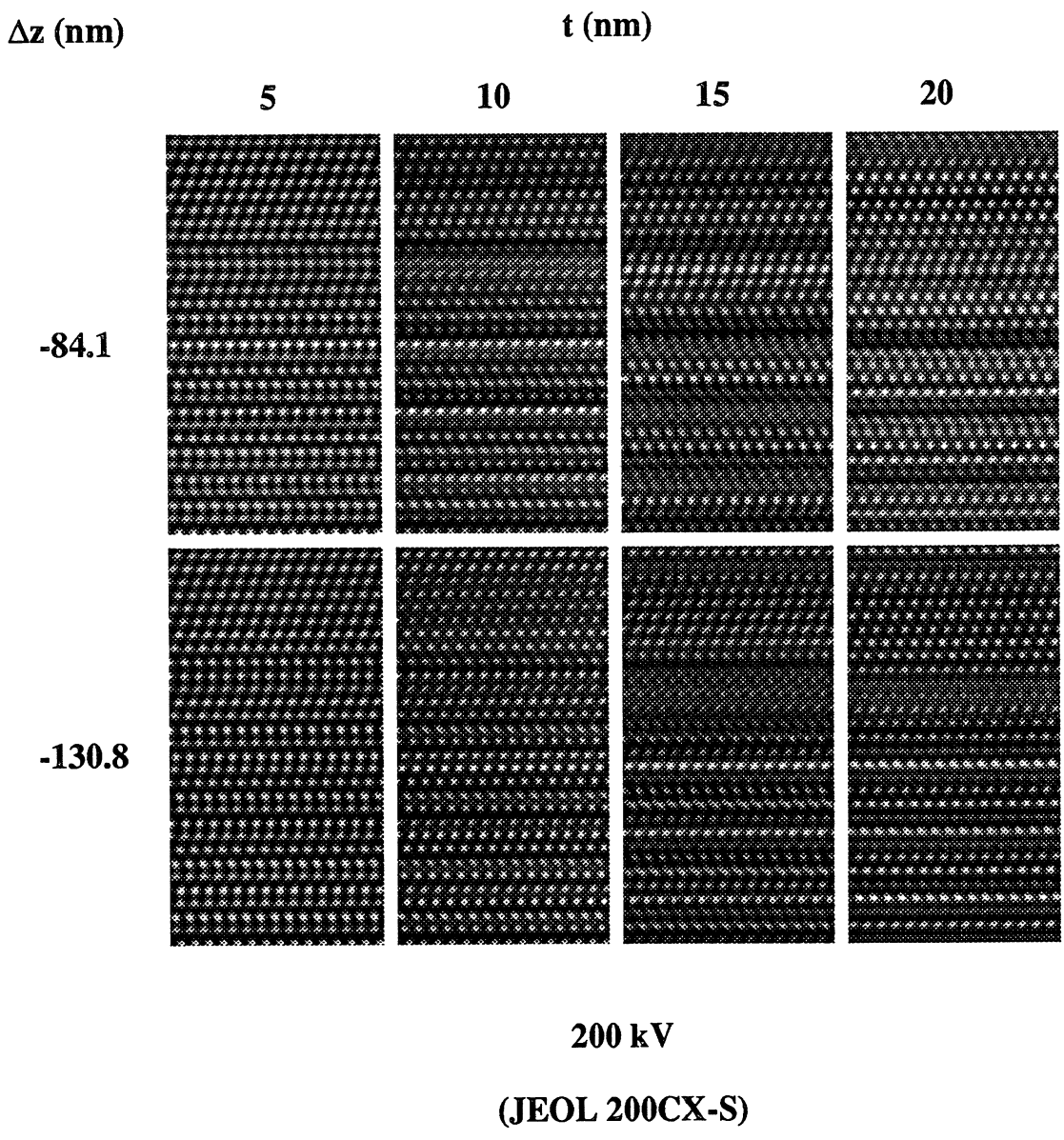

Fig. 7. — Simulated images for the structure shown in figure 6 for the JEOL 200CX-S microscope (voltage $V = 200$ kV; spherical aberration $C_S = 2$ nm; beam divergence (half-angle) $\delta\theta = 0.603$ mard; focus spread (rms) $\delta z = 7.1$ nm; objective aperture cut-off at a frequency $u = 0.8$ Å^{-1}). Different thicknesses (t) and defocus values (Δz) corresponding to the two first broad passbands of the microscope have been considered.

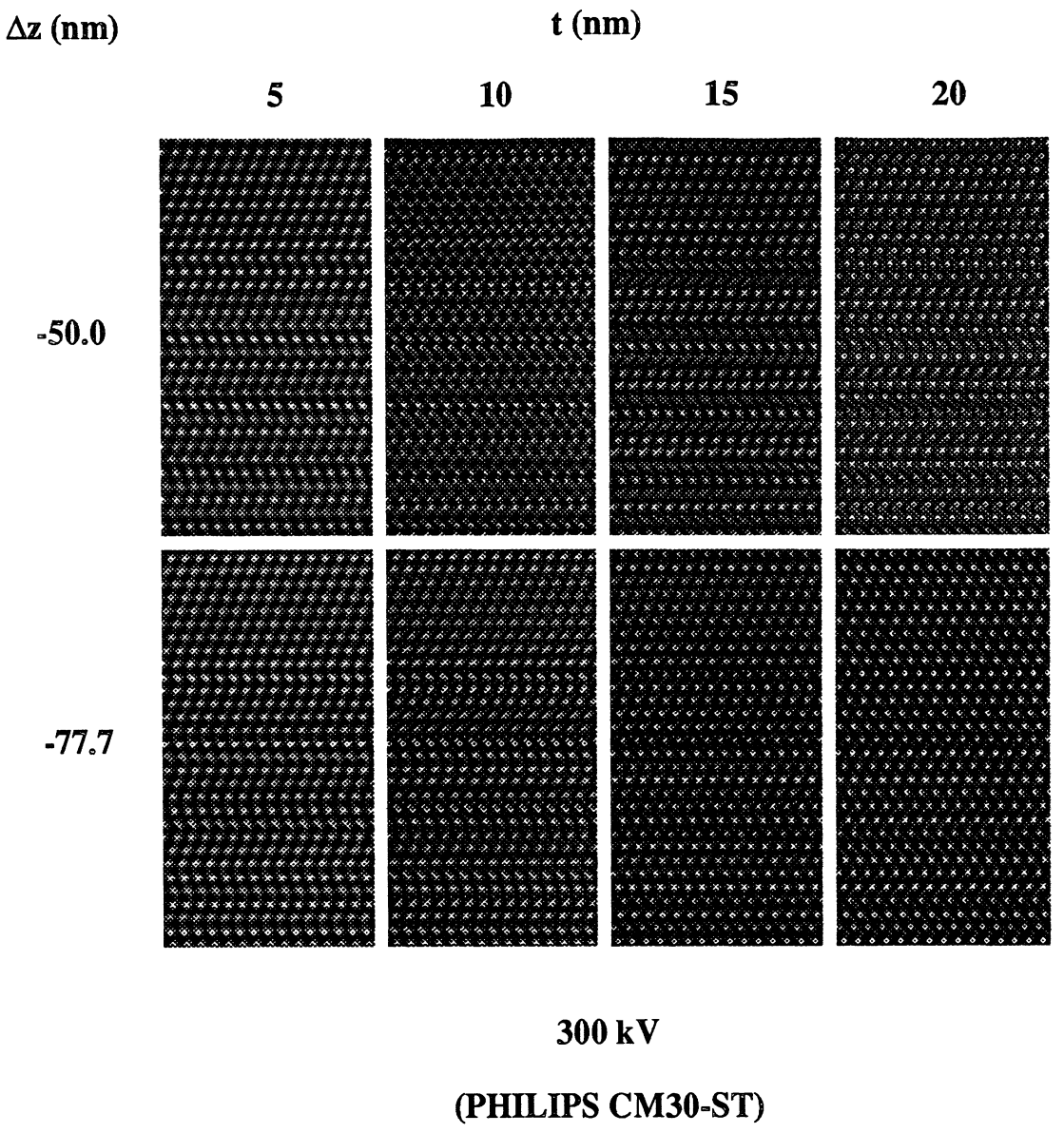

Fig. 8. — Simulated images of the structure of figure 6 for the PHILIPS CM30-ST microscope (voltage $V = 300$ kV; spherical aberration $C_S = 0.9$ nm; beam divergence (half-angle) $\delta\theta = 0.64$ mrad; focus spread (rms) $\delta z = 5.4$ nm; objective aperture $u = 0.8$ Å^{-1}). Same thicknesses (t) as in figure 7. The values of the defocus (Δz) also corresponds to the two first passbands.

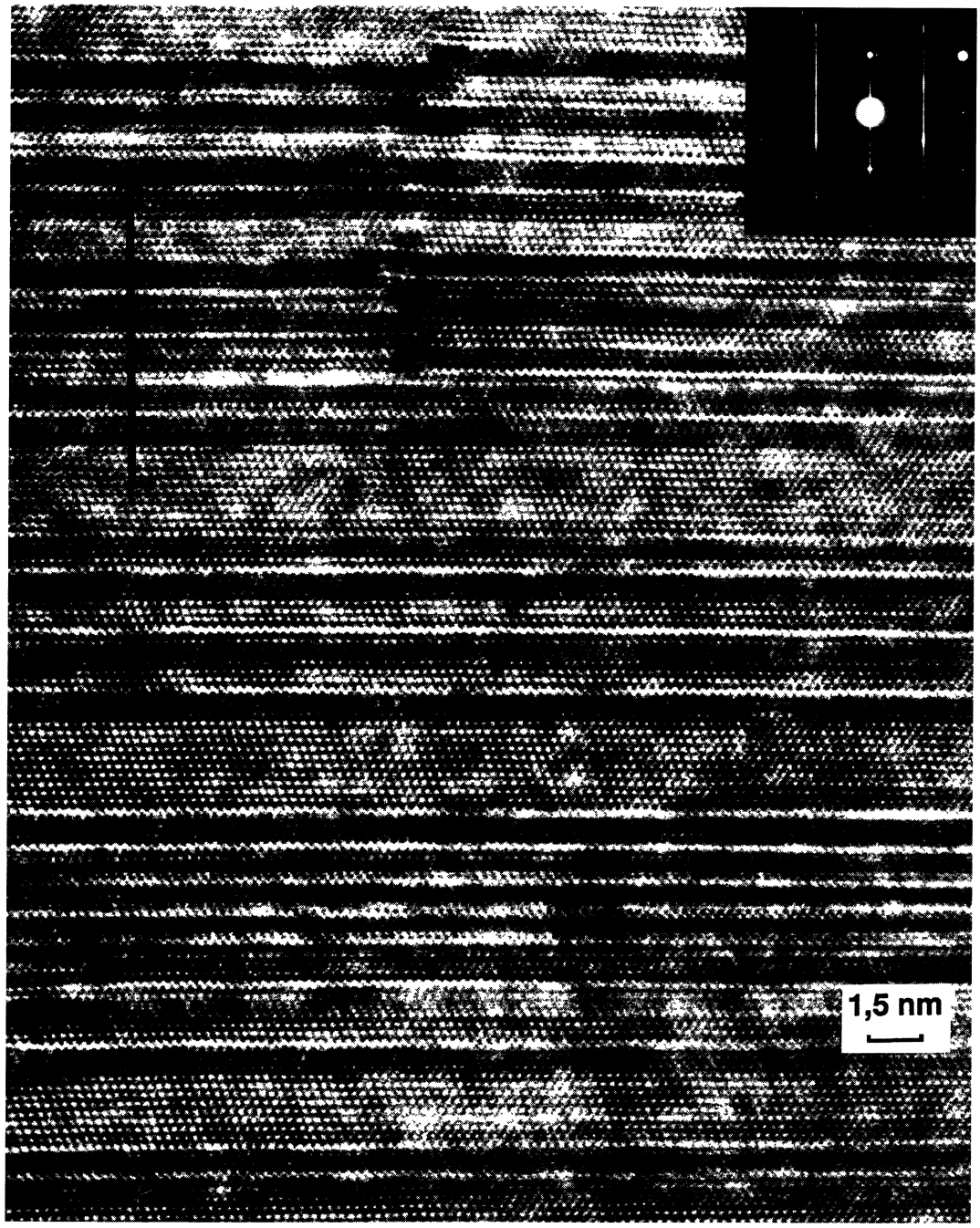

Fig. 9. — JEOL 200CX-S high resolution image of a SiC(CVI) crystal. Blurred bands prevent the identification of the polytype.

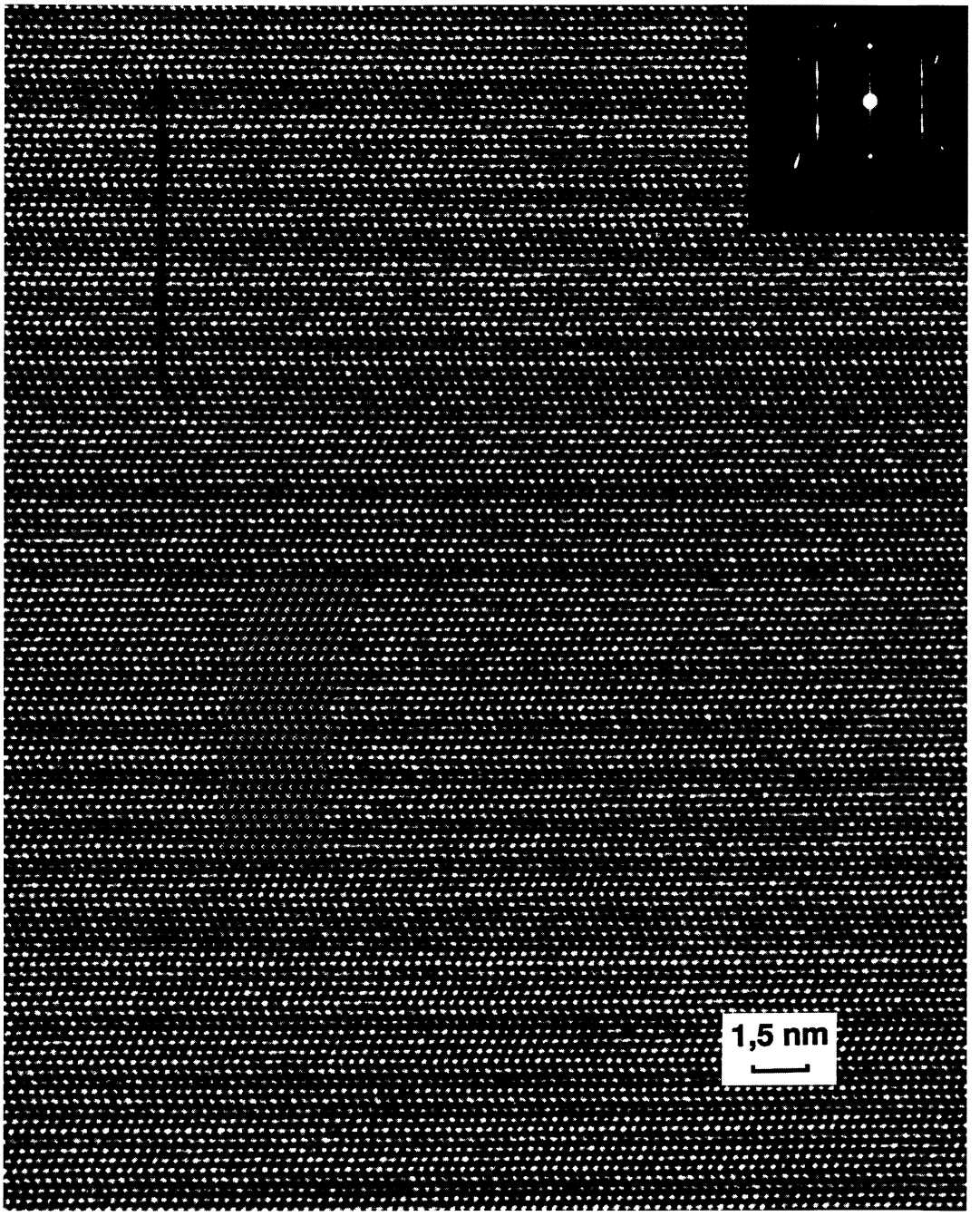

Fig. 10. — PHILIPS CM30-ST high resolution image of a SiC(CVI) crystal. The white dots can be directly correlated with the SiC atomic bicolumns (see Fig. 1). No periodicity is observed in the stacking so that the structure indicates a "one-dimensionally-disordered" polytype.

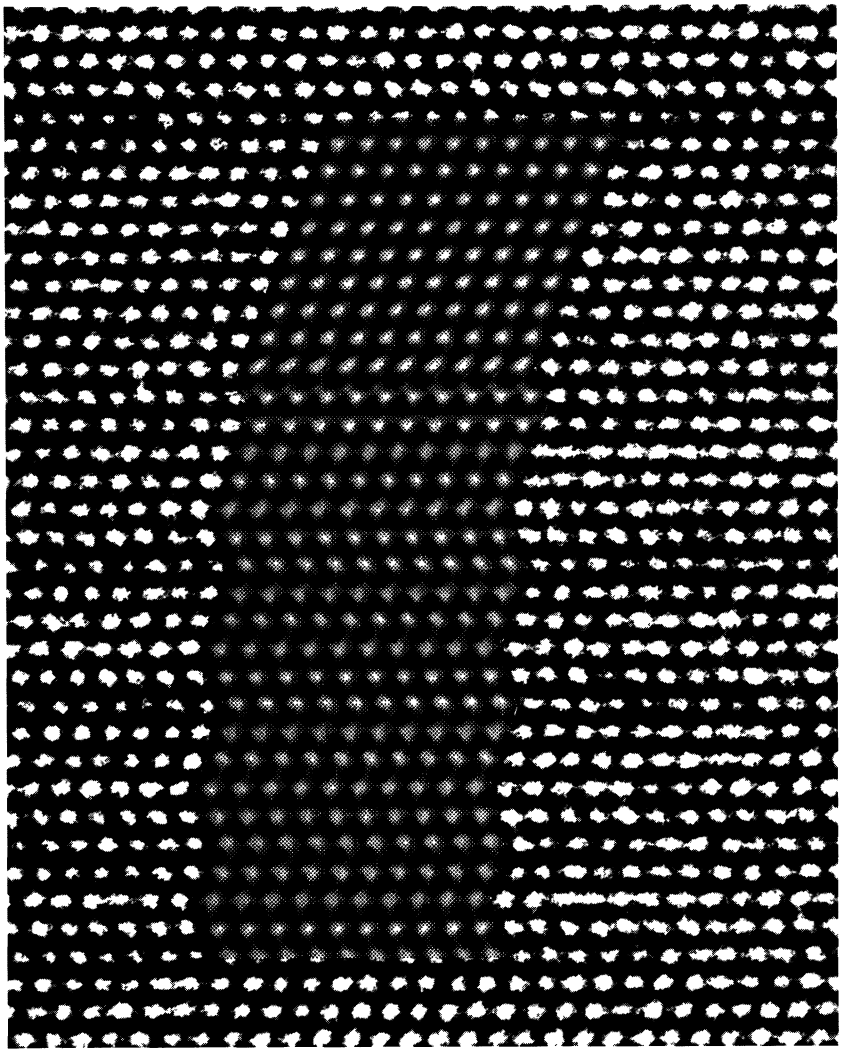

Fig. 11. — Enlargement of figure 10 where the good matching between the experimental and the calculated images of the structure of figure 6 is striking.

References

[1] NASLAIN R., ROSSIGNOL J.Y., QUENISSET J.M., LANGLAIS F., Introduction aux matériaux composites, volume 2, R.Naslain (CNRS Ed., 1985) p. 439.

[2] AYACHE J., BONNAMY S., BOURRAT X., DEURBERGUE A., MANIETTE Y., OBERLIN A., BACQUE E., BIROT M., DUNOGUES J., PILLOT J-P., *J. Mater. Sci. Lett.* **7** (1988) 885.

[3] MANIETTE Y., OBERLIN A., *J. Mater. Sci.* **24** (1989) 3361.

[4] MANIETTE Y., Thesis, Université de Pau et des Pays de l'Adour (1988).

[5] LOB N., LANCIN M., THIBAULT-DESSEAUX J., TREBBIA P., communication SFME 1990.

[6] CHRISTIN F., NASLAIN R., BERNARD, Actes Conf. Int. CVD-7, T.O. Seedwick and H.Lydtin Eds., Los Angeles 1979 (The Electrochem. Soc., Princeton, 1979) p. 499.

[7] SPENCE J.C.H., Experimental high resolution microscopy, 2nd ed. (Oxford University Press, 1988).

[8] JEPPS N.W., SMITH D.J., PAGE T.F., *Acta Cryst.* **A35** (1979) 916.
[9] JEPPS N.W., PAGE T.F., *J. Microsc.* **119** (1980) 177.
[10] SINGH G., RAI R.S., *Bull. Mater. Sci.* **6** (1984) 459.
[11] VAN TENDELOO G., *Mat. Res. Soc. Symp. Proc.* **31** (1984) 279.
[12] LANCIN M., THIBAULT-DESSEAUX J., *J. Phys. Colloq. France* **49** (1988) C5-305.
[13] EGERTON R.F., Electron Energy Loss Spectroscopy in the electron microscope (Plenum Press Ed., New-York, 1986).
[14] YESSIK M., SHINOZAKI S., SATO H., *Acta Cryst.* **A31** (1975) 764.
[15] KHUO C.L., ZHOU J., YE H.Q., KHUO K.H., *J. Appl. Cryst.* **15** (1982) 199.
[16] RAI R., SINGH S.R., DUBEY M., SINGH G., *Bull. Minéral.* **109** (1986) 509.
[17] SATO H., SHINOZAKI S., *Mat. Res. Bull.* **10** (1975) 257.
[18] SHINOZAKI S., SATO H., *J. Am. Ceram. Soc.* **61** (1978) 425.
[19] SHINOZAKI S., KINSMAN K.R., *Acta Met.* **26** (1978) 769.
[20] SMITH D.J., O'KEEFE M.A., *Acta Cryst.* **A39** (1983) 139.
[21] O'KEEFE M.A., KILAAS R., *Scanning Microscopy Suppl.* **2** (1988) 225.
[22] SCHAMM S., MAZEL A., DORIGNAC D., SEVELY J., Matériaux composites pour applications à hautes températures, R. Naslain *et al.* Eds., AMAC/CODEMAC (1990) p. 207.
[23] SMITH D.J., BURSILL L.A., WOOD G.J., *Ultramicroscopy* **16** (1985) 19.